Non-Stationary Finite-Amplitude Convection in a Thin Fluid Layer Bounded by a Stably Stratified Region

YOSHIMITSU OGURA AND AKIKO YAGIHASHI[1]

Laboratory for Atmospheric Research, University of Illinois, Urbana

(Manuscript received 15 April 1971, in revised form 2 August 1971)

ABSTRACT

Numerical integrations are performed for the equations governing two-dimensional convection flows in a fluid confined between two horizontal plates. A situation considered here is that local heating at a time-independent rate is provided at the middle level of the fluid so that the upper half of the fluid is destabilized and the lower half stabilized. It is shown that steady-state solutions are obtained when the Rayleigh number (R) is 1.1 times Rc (critical Rayleigh number at which convection sets in according to the linearized theory). For three cases where R=1.5 Rc, 2 Rc and 3 Rc, time-dependent solutions are obtained which describe extremely regular and repeatable convection flows. The flow pattern is such that plume-like cells generated by heating move horizontally, merge with neighboring plumes, and new plumes are generated. This process is repeated. Time-dependent but irregular solutions are obtained for R=5 Rc and beyond.

1. Introduction

In the classical Bénard-Rayleigh convection problem, a layer of fluid is bounded above and below by horizontal boundaries which are maintained at constant temperatures. When the temperature difference between the two boundaries (or more generally the Rayleigh number) exceeds a critical value, buoyancy-generated convection motions take place. It has been well established that the flow thus generated maintains a steady state when the supercritical Rayleigh number is not too high. Latest references include Koschmieder (1969) and Krishnamurti (1970) for experimental investigations and Foster (1969) and Ogura (1971) for numerical works where the two-dimensional governing equations are numerically integrated as an initial-boundary value problem (see Section 6 for more references).

The behavior of the fluid is different, however, when a destabilized fluid layer is bounded by one or more stabilized layers. Consider a fluid layer in which an internal heat source is distributed so that an unstable density stratification is maintained in the upper portion of the fluid and a stable stratification is maintained in the lower portion. It is observed that the flow induced in the fluid exhibits quite regular periodic variations with time when the Rayleigh number evaluated in terms of the parameters for the destabilized layer exceeds a certain critical value, even with heating at the time-independent rate of heating.

This interesting type of convection was first observed[2] in the laboratory experiments by Whitehead and Chen (1970) and Kimura (unpublished paper) independently. Ogura and Yagihashi (1970) have also demonstrated the existence of a similar type of convection by integrating numerically the governing equations. Due to the limitiation of computer time available, however, Ogura and Yagihashi discussed only the cases where the number of degrees of freedom for these motions were extremely limited.

In real geophysical and astrophysical fluids, it is more common for destabilized layers to be bounded by stabilized fluid layers rather than having destabilized layers bounded by rigid boundaries with infinite heat conductivity, as postulated in the classical Bénard-Rayleigh problem. This hydrodynamic interest is the motivation to repeat a numerical investigation of the convection motion in the destabilized fluid layer lying below the stabilized layer, taking, however, much finer spatial resolutions in the numerical integration than those taken previously by Ogura and Yagihashi (1970). The result obtained in this work indicates that periodic convection takes place at a much lower Rayleigh number than that found previously.

2. Governing equations

We use the coordinate system which has the z axis in the vertical and the y axis horizontal (Fig. 1).

[1] Present affiliation: Ocean Research Institute, University of Tokyo.

[2] According to Martin (1967), Watson (1966) observed temperature oscillations in a fluid confined in a closed vertical cylinder with internal heat generation. However, Watson's paper was not available to the authors.

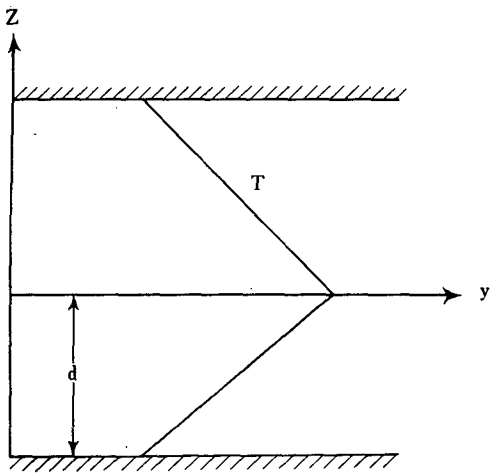

FIG. 1. Coordinate system and fluid layer for the numerical experiment.

Two-dimensional motion in the y,z plane will be considered in a fluid layer confined between two horizontal plates at $z=d$ and $z=-d$ which are maintained at the same time-independent temperature. A thin layer at the middle of the fluid is heated uniformly at a constant rate $Q(z)$.

With the Boussinesq approximation, the equations for vorticity in the direction perpendicular to the y,z plane and temperature variations are written as

$$\frac{\partial \xi}{\partial t}+v\frac{\partial \xi}{\partial y}+w\frac{\partial \xi}{\partial z}=\alpha g\frac{\partial T}{\partial y}+\nu\nabla^2\xi, \tag{2.1}$$

$$\frac{\partial T}{\partial t}+v\frac{\partial T}{\partial y}+w\frac{\partial T}{\partial z}=\kappa\nabla^2 T+\frac{Q}{c_p\rho_0}, \tag{2.2}$$

with

$$\xi=\frac{\partial w}{\partial y}-\frac{\partial v}{\partial z}=\nabla^2\psi,$$

and where v, w are the velocity components along the y and z axes, respectively, ψ the streamfunction, T the temperature, t the time, ρ_0 a constant fluid density, ν the kinematic viscosity, κ the thermal diffusivity, α the coefficient of volume expansion, g the acceleration of gravity, c_p the specific heat at constant pressure, and $\nabla^2=\partial^2/\partial y^2+\partial^2/\partial z^2$.

For the convenience of numerical analysis, we divide the temperature field $T(y,z,t)$ into two parts, $\bar{T}_Q(z)$ which will be defined in Eq. (2.4) and the deviations from $\bar{T}_Q(z)$:

$$T(y,z,t)=\bar{T}_Q(z)+\theta(y,z,t), \tag{2.3}$$

where (2.2) implies that $\bar{T}_Q(z)$ must satisfy the equation

$$0=\kappa\frac{d^2\bar{T}_Q}{dz^2}+\frac{Q}{c_p\rho_0}. \tag{2.4}$$

The equation for θ is then derived as

$$\frac{\partial \theta}{\partial t}+v\frac{\partial \theta}{\partial y}+w\left(\frac{\partial \theta}{\partial z}+\frac{d\bar{T}_Q}{dz}\right)=\kappa\nabla^2\theta. \tag{2.5}$$

Note that the effect of the internal heating introduced to the fluid layer is now represented by the term $d\bar{T}_Q/dz$.

We consider the vertical distribution of heat source $Q(z)$ as expressed by

$$Q(z)=Q_0\delta(z),$$

where $\delta(z)$ is the Dirac delta function and Q_0 a constant. The distribution of $\bar{T}_Q(z)$ resulting from this $Q(z)$ is such that it has a constant positive vertical gradient (denoted by β) in the layer below $z=0$ and a constant negative gradient $-\beta$ in the layer above $z=0$.

Eqs. (2.1) and (2.5) are non-dimensionalized by using d, d^2/κ and βd as scale factors for length, time and temperature. Hereafter, all quantities should be understood to be expressed in non-dimensional form, unless otherwise stated. Eqs. (2.1) and (2.5) are then written as

$$\frac{\partial \xi}{\partial t}+v\frac{\partial \xi}{\partial y}+w\frac{\partial \xi}{\partial z}=\mathrm{PrR}\frac{\partial \theta}{\partial y}+\mathrm{Pr}\nabla^2\xi, \tag{2.6}$$

$$\frac{\partial \theta}{\partial t}+v\frac{\partial \theta}{\partial y}+w\left(\frac{\partial \theta}{\partial z}+\beta^*\right)=\nabla^2\theta, \tag{2.7}$$

$$\xi=\nabla^2\psi, \tag{2.8}$$

where

$\mathrm{R}=\alpha g\beta d^4/\kappa\nu$: Rayleigh number

$\mathrm{Pr}=\nu/\kappa$: Prandtl number

and

$$\beta^*=\begin{cases}-1, & \text{for} \quad 0<z<1\\ 0, & \text{at} \quad z=0\\ 1, & \text{for} \quad -1<z<0\end{cases} \tag{2.9}$$

We shall apply the free boundary conditions at both top and bottom of the fluid which demand

$$\theta=\psi=\nabla^2\psi=0.$$

As discussed by Whitehead and Chen (1970), there are a number of possible alternatives in defining the Rayleigh number in the present problem. The definition adopted above has an advantage that it is directly related to the given external parameter $Q(z)$. The disadvantage may be, as was shown previously (Ogura and Yagihashi, 1970), that the horizontally averaged temperature difference between the heated layer and the top of the fluid differs considerably from β^* when finite-amplitude convection motions are taking place. This temperature difference is not known *a priori*.

The lateral boundary conditions we use are that all variables are cyclic over the interval L in the y direction. The fundamental wavelength L we selected in

this work is twice the critical wavelength. Several articles were published in which linear stability analyses were performed for the onset of motions in a destabilized layer lying below a stabilized layer. The critical Rayleigh number was determined as a function of the ratio of the depths of the destabilized and stabilized layers and of the ratio of vertical temperature gradients in the two layers (Gribov and Guervich, 1957; Veronis, 1965; Rintel, 1967; Whitehead and Chen, 1970; Ogura and Kondo, 1970).

For the convenience of discussions which follow, the stability curve calculated by Ogura and Kondo (1970) is reproduced in Fig. 2 for the case which corresponds to the temperature distributions as represented by (2.9). In Fig. 2, the abscissa a is the horizontal wavenumber non-dimensionalized by the factor d. We observe that the critical Rayleigh number (hereafter denoted as Rc) is approximately 225 and the critical wavenumber is approximately 1.5. The horizontal dimension L of our fluid is selected to be 8.4 so that, as will be shown in Fig. 4, two pairs of convection cells are present at the Rayleigh number just above Rc.

It may be remarked here that the results which will be described for the temperature distribution given by Eq. (2.9) are essentially unchanged if the temperature gradients are reversed (that is, $\beta^*=1$ for $0<z<1$ and $\beta^*=-1$ for $-1<z<0$) with the Boussinesq approximation we applied.

3. Numerical integrations

The numerical method used to integrate Eqs. (2.6), (2.7) and (2.8) as an initial and boundary-value problem is the same as that used in the previous study (Ogura and Yagihashi, 1969). The prognostic equations (2.6) and (2.7) are integrated using the finite-difference schemes proposed by Lilly (1964) except for the diffusion terms which are evaluated by using the DuFort-Frankel scheme. The system used here preserves the total energy of the system and the variance of temperature in the finite-difference form in a manner analogous to that of the continuous systems. Poisson's equation (2.8) is solved directly by Fourier decomposition in the y direction and by using the algorithm for solutions for one-dimensional two-point boundary value problems, as described by Todd (1962, p. 394) or Richtmyer and Morton (1967, p. 198). With the application of the Fast Fourier Transform algorithm for trigonometric decomposition and synthesis, the solutions of the Poisson's equation are found to be obtained with sufficient accuracy and efficiency (Ogura, 1969).

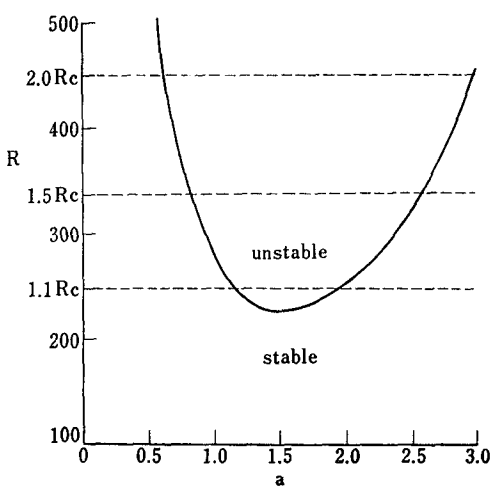

FIG. 2. The marginal stability curve derived from the linear stability problem (Ogura and Kondo, 1970) corresponding to the temperature distribution in Fig. 1.

TABLE 1. Specifications of seven cases investigated.

Case no.	R/Rc	Time span	Result	Period
1	1.1	180	Steady	...
2	1.5	176	Regular time dependent	317.2
3	2.0	140	Regular time dependent	131.2
4	3.0	58	Regular time dependent	58.2
5	5.0	13.6	Irregular time dependent	...
6	10.0	4.8	Irregular time dependent	...
7	20.0	4.8	Irregular time dependent	...

The two-dimensional domain was divided into a mesh of 32 (horizontal)×20 (vertical). Different time increments Δt were used to permit the integration to proceed without any computational instability. In our numerical approach, the calculation begins with no convective motion but with an initial uniform supercritical vertical temperature gradient [Eq. (2.9)]. Motion is initiated by introducing a random perturbation of the order of 1/100 in magnitude into the temperature field.

On the Control Data 6600 Computer at the National Center for Atmospheric Research, it took about 225 msec for each time step iteration.

In all cases, the Prandtl number was given a value of 0.713 corresponding to air.

4. Results

Table 1 summarizes the results of numerical integrations for the seven cases investigated. We observe that three different types of convection motions take place, depending upon the Rayleigh number. These are described in the following subsections.

a. Steady motion

Fig. 3 shows the variations with time of temperature observed at one of the grid points ($y=4.2$ and $z=0.5$) and the non-dimensional vertical heat flux (Nusselt number) evaluated at $z=0.5$ for R=1.1 Rc (case 1). It can be seen that the motion attains an approximate steady state at approximately $t=70$ and remains in that steady state until the time of termination of the integration ($t=180$).

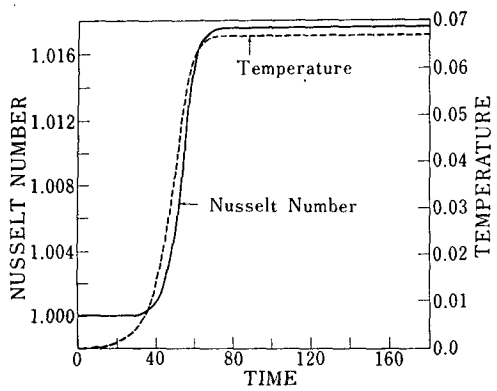

FIG. 3. Variations with time of the Nusselt number at $z=0.5$, and temperature at a grid point for R=1.1 Rc (case 1).

Fig. 4 shows the fields of temperature and streamfunction at $t=180$. As predicted by the linear theory, two pairs of cells are established. It may be noted, as shown in the bottom figure of Fig. 4, that the motion is not confined in the upper destabilized layer but penetrates deeply into the lower stabilized layer. Another interesting feature in Fig. 4 is that in the downdraft region, say at $z=-0.3$, w is about $\frac{2}{3}$ as intense as at $z=0.3$ and yet the temperature deviation induced there at $z=-0.3$ is only about $\frac{1}{5}$ of that at $z=0.3$. This deep penetration and the small temperature deviation in the penetrated region are consistent with those described in terms of the eigenfunctions for unstable modes [see Fig. 10 of Ogura and Kondo (1970)].

b. Regular time-dependent motion

With increasing Rayleigh number, the motion begins to exhibit quite regular periodic variations with time. Examples are given in Fig. 5 which shows the variations with time of the temperature at the grid points ($y=2.44$ and $z=0.5$) and the Nusselt number evaluated at $z=0.5$ respectively for R=2 Rc (case 3).

The most striking feature observed in these figures is that, after an initial phase of a certain length of time, the motion remains in a quasi-steady state for a relatively long period of time and then, after experiencing a rapid transition stage, settles at another quasi-steady state. This variation is then repeated.

Fig. 6 shows the fields of temperature and streamfunction at several instances. Perhaps we can show best what is taking place in the fluid by Fig. 7 in which the continuous sequence of the horizontal distribution

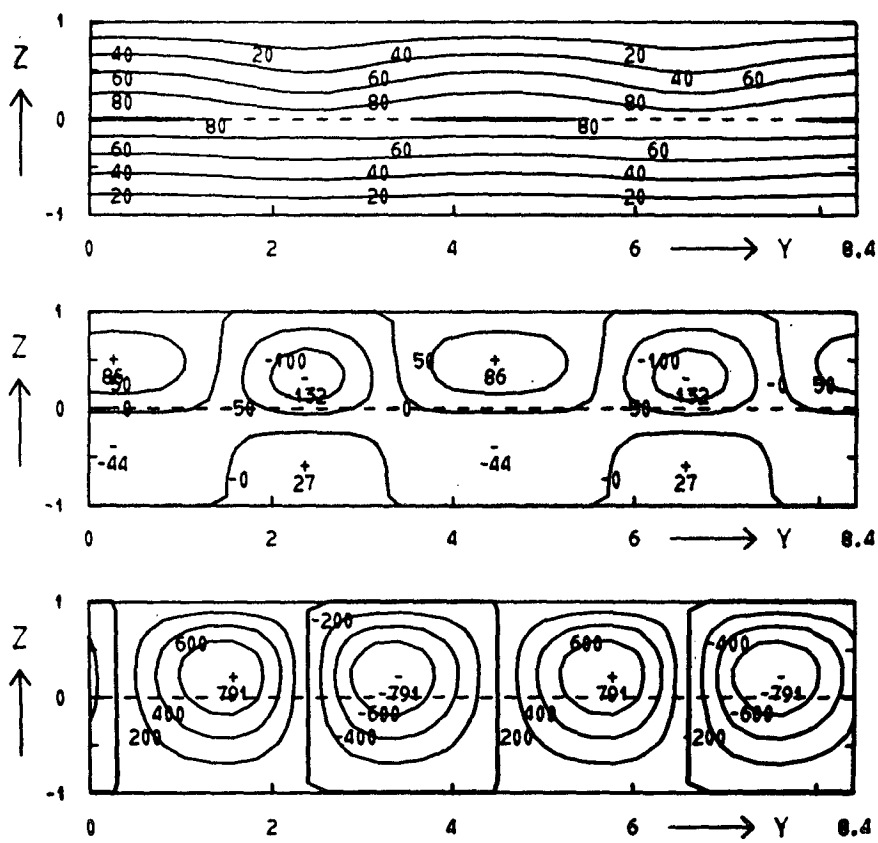

FIG. 4. The steady-state fields of temperature and streamfunction at $t=180$ for R=1.1 Rc (case 1): upper, temperature in units of 10^{-2}; middle, temperature deviations from the horizontal average in units of 10^{-3}; lower, streamfunction in units of 10^{-3}.

of temperature deviation θ at $z=0.5$ is shown. It is to be noted that the range of the y coordinate in Fig. 7 is wider than that actually used in the numerical computation. This was done for the convenience of illustration and by using the cyclic behavior of the motion over the range of 8.4. During the period roughly from $t=95$ to $t=120$, two plumes with negative temperature deviations are present and remain in a quasi-steady state (Fig. 6a), more or less in a similar fashion to that observed in the case of R=1.1 Rc (Fig. 4). At approximately $t=120$, the left plume begins to move to the left and the right plume to the opposite direction (Fig. 6b). By approximately $t=130$, a new plume is established at the location right between the two old plumes which meanwhile merge to form a new single plume (Fig. 6c). This completes a quarter cycle. The rest of the cycle is shown in Fig. 7 which covers approximately an entire cycle. The period[3] of a complete cycle in this case 3 is 131.2.

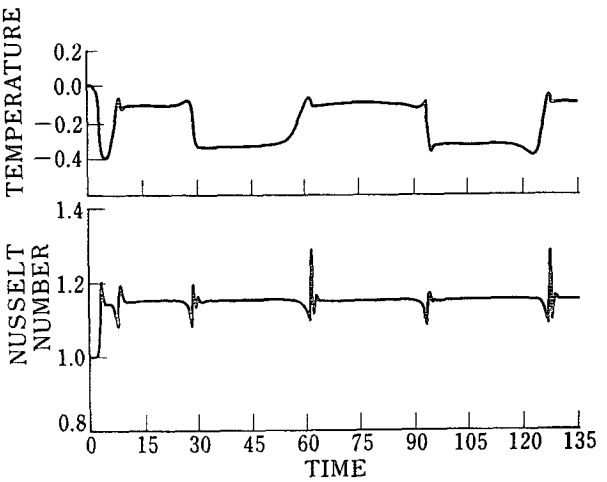

FIG. 5. Variations with time of the Nusselt number at $z=0.5$ and temperature at a grid point for R=2 Rc (case 3).

In Fig. 8, the periods thus determined are plotted against the Rayleigh number for the three cases 2, 3 and 4. The general tendency of the curve is that the period increases as the Rayleigh number decreases. It appears that the period becomes infinity as the Rayleigh

[3] The non-dimensional Brunt-Väisälä frequency for the stably stratified layer is given by $(RPr)^{\frac{1}{2}}$ in the present case. With R=2 Rc=450 (case 3) and Pr=0.713, the period of Brunt-Väisälä oscillations is approximately 0.35, much shorter than that observed here. The time-dependent oscillations therefore appear to be basically due to nonlinearities and not gravity oscillations excited in the stable region which affect the unstable region.

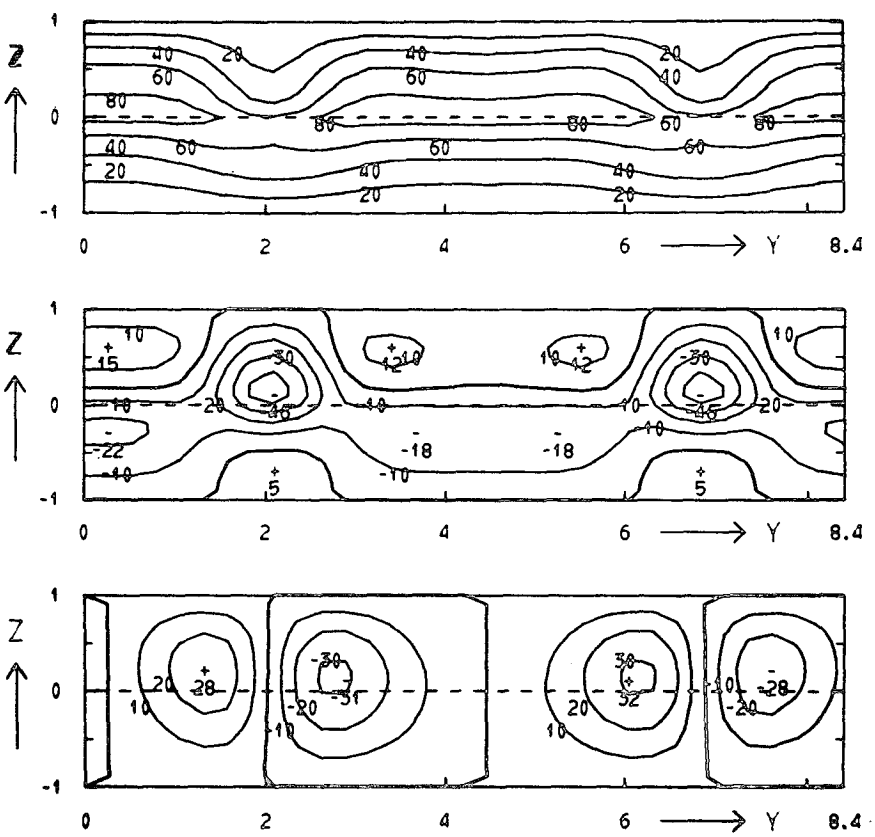

FIG. 6a. The fields of temperature (upper diagram), temperature deviation from the horizontally averaged temperature (middle diagram), and streamfunction (lower diagram) for R=2 Rc (case 3) at $t=124.0$.

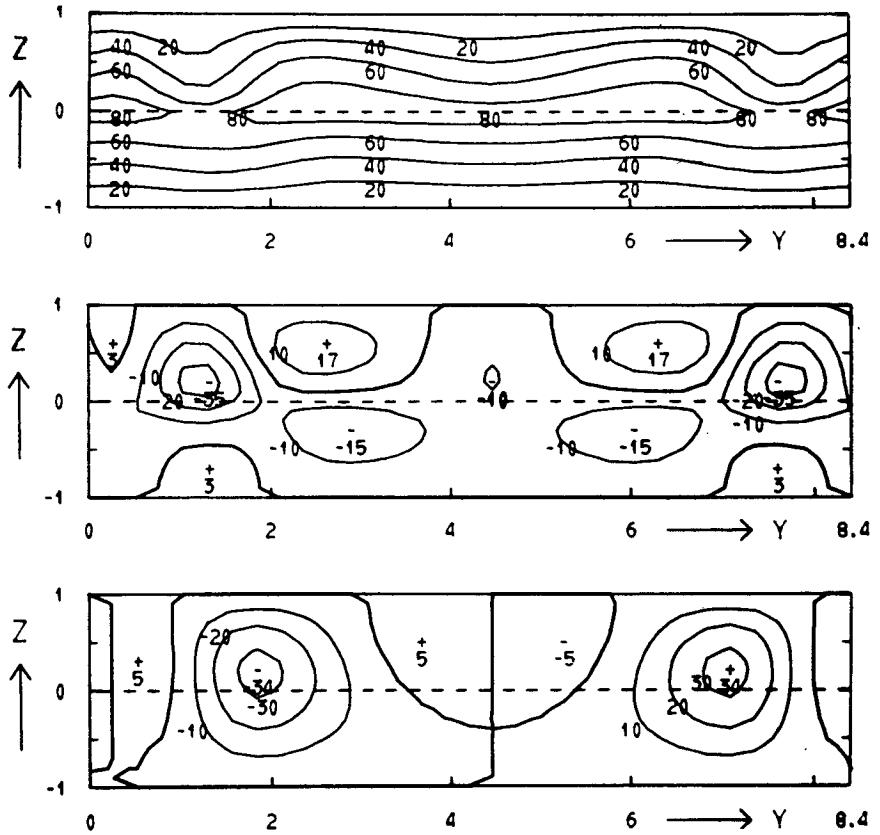

FIG. 6b. Same as 6a except for $t=126.8$.

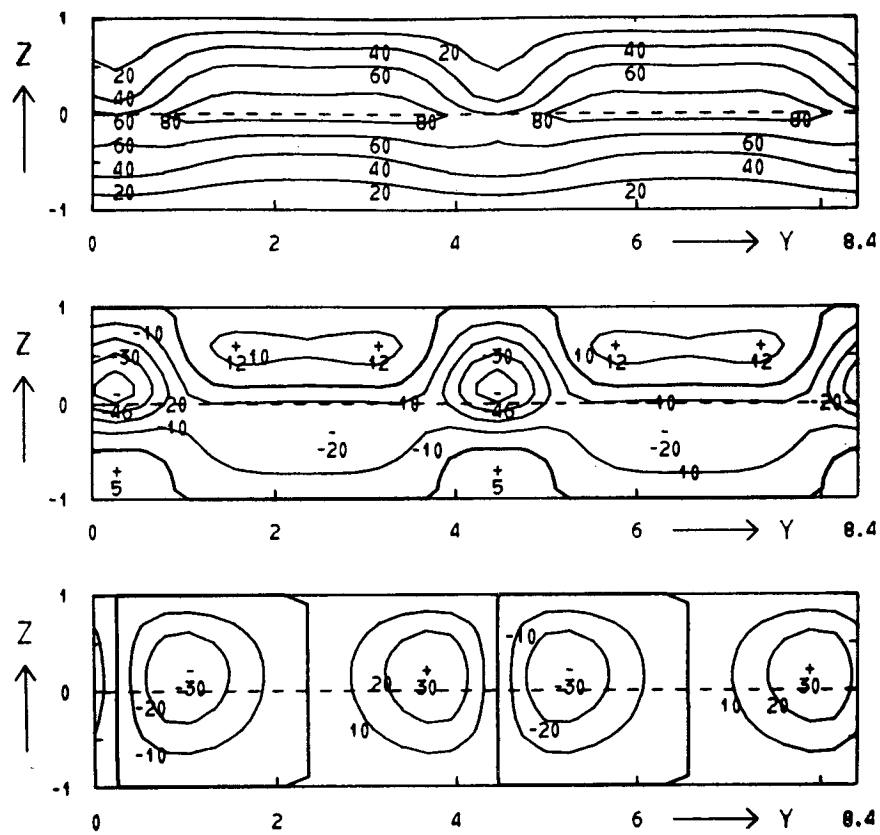

FIG. 6c. Same as 6a except for $t=129.6$.

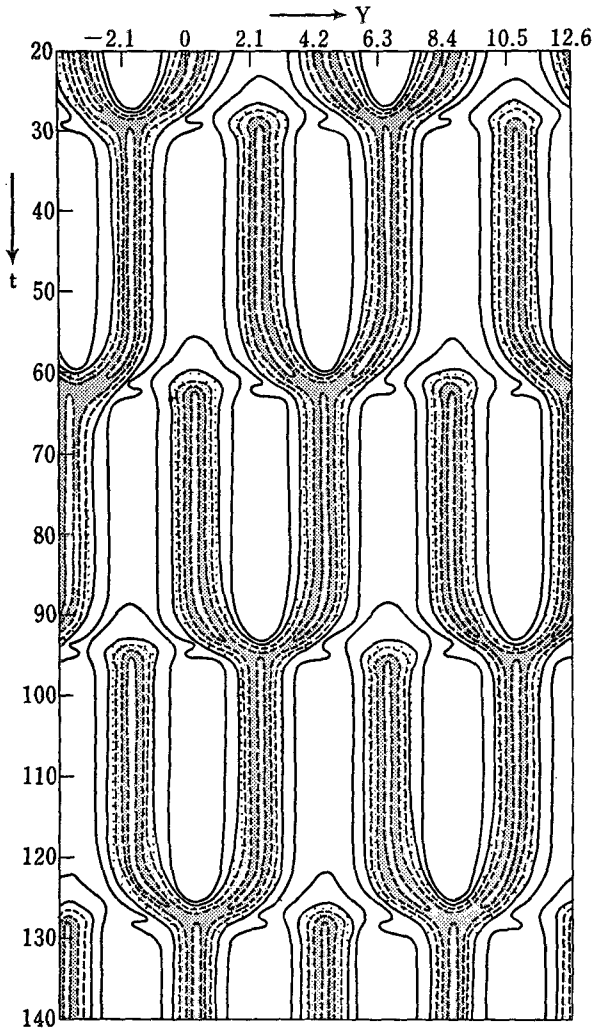

FIG. 7. The variation of horizontal temperature distribution with time at $z=0.5$. The isotherms are at an interval of 0.1.

number approaches Rc. If this is the case, the steady-state motion observed for R = 1.1 Rc may be more properly described as a periodic motion with an extremely long period.

In our previous paper (Ogura and Yagihashi, 1970) it was found that periodic convection takes place only when the Rayleigh number is increased to approximately 38 Rc for a fluid system with a very limited number of degrees of freedom.[4] The fact that it is found in the present study that a periodic motion takes place with a Rayleigh number $\lesssim 1.5$ Rc may indicate that the periodic motion represents a preferred

[4] In that truncated system, only three horizontal modes were retained ($k=0.5$, 1.5 and 2.0) whereas 16 modes should be resolved in principle in the present study with 32 grid points in the horizontal direction ($k=0.75$, 1.5, 2.25, 3.0, ...). The vertical resolutions are the same for both cases. As will be shown later, almost all kinetic energy is distributed in the mode $k=1.5$ and its bi-harmonics during the quasi-steady period for R = 2 Rc, for example. No bi-harmonics were present in the previous case.

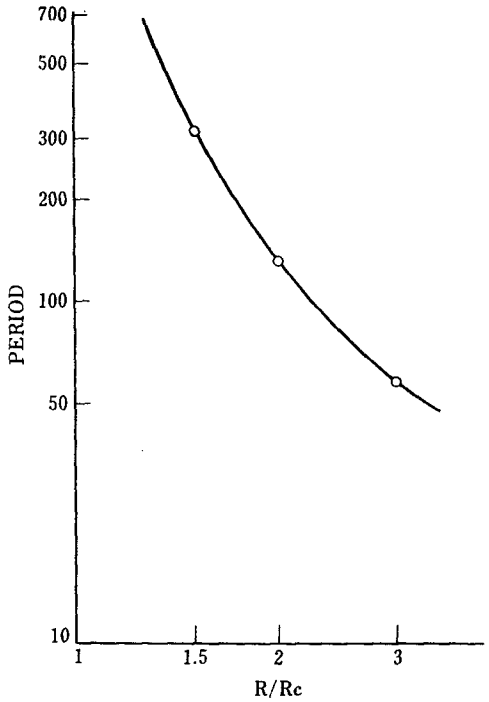

FIG. 8. Period of oscillations as a function of the Rayleigh number.

mode of convection for a destabilized layer lying above a stabilized layer at a slightly supercritical Rayleigh number.

c. Irregular time-dependent motion

When the Rayleigh number goes up to 5 Rc, the motion becomes more irregular. An example is shown in Fig. 9. The flow pattern in this case consists of the horizontal translation, generation and amalgamation of plumes as in case 3 but in a more chaotic fashion.

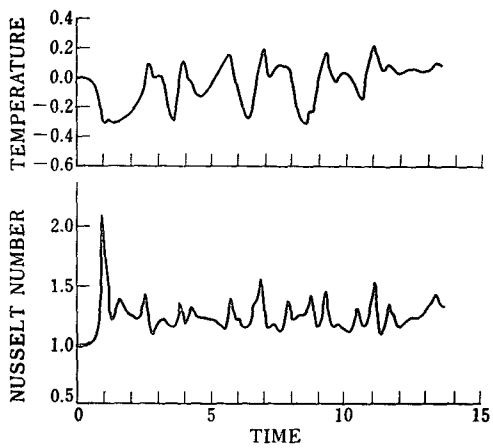

FIG. 9. Variations with time of the Nusselt number at $z=0.5$ and temperature at a grid point for R = 5 Rc (case 5).

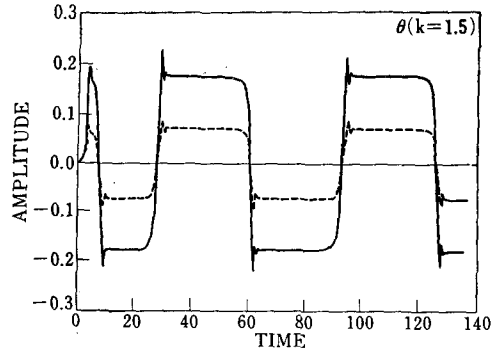

FIG. 10. Variations with time of the amplitudes of cosine (solid line) and sine (dashed line) harmonics with $k=1.5$ for temperature deviations at R=2 Rc (case 3).

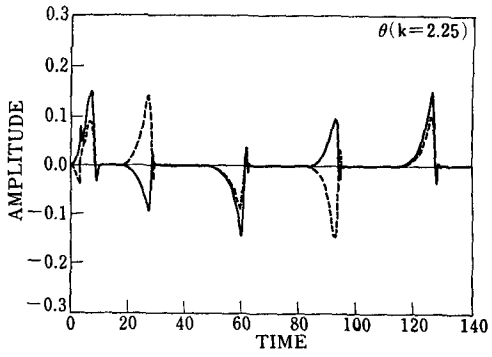

FIG. 12. Same as Fig. 10 except for $k=2.25$.

5. Harmonic representation

In order to get a better understanding of the physical process involved in periodic convection, the following harmonic decomposition in the y direction was performed for the computed fields of temperature and streamfunction at $z=0.5$:

$$\psi(y,t)=\sum_k \psi_k(y,t)$$

$$=\sum_k \Psi_k^s(t)\sin ky+\sum_k \Psi_k^c(t)\cos ky,$$

$$\theta(y,t)=\sum_k \theta_k(y,t)$$

$$=\sum_k \Theta_k^s(t)\sin ky+\sum_k \Theta_k^c(t)\cos ky,$$

where $k=(a_c/2)n$, $n=0, 1, 2, \ldots$, and a_c denotes the critical wavenumber ($a_c=1.5$). Figs. 10–13 give some examples of the variation of the amplitudes with time for the case of R=2 Rc (case 3).

Close inspection of the result indicates that it is convenient for discussion to classify all harmonics into two groups, because these two groups have distinctively different dynamic characteristics, as will be indicated below. The first group, which we call group A hereafter, consists of the harmonics of $k=0$, the critical wavenumber a_c and the bi-harmonics of a_c ($k=3$, 4.5, 6, . . .). The remaining harmonics ($k=0.75$, 2.25, 3.75, 5.25, . . .) constitute the other group (group B). Figs. 10 and 11 represent a typical example for group A and Figs. 12 and 13 an example for group B.

Table 2 gives the total amplitudes (square roots of the sum of the squared amplitudes) of the lowest nine harmonics of the temperature field for the quasi-steady state in case of R=2 Rc (case 3). For comparison, the spectral density distribution for case 1 where the motion attains a steady state is also included in Table 2. We immediately observe that the amplitudes for group A at the quasi-steady state is consistently much larger than those for group B, as is the case in the steady-state solution (case 1). In other words, the fields of temperature and streamfunction in the quasi-steady state consist almost exclusively of the harmonics of a_c and its bi-harmonics.

Near the end of each period in the quasi-steady state, the amplitudes of group A diminish, while those of group B increase very rapidly. Their growth with time are in fact well represented by exponential functions. At their peaks, the total amplitudes of harmonics of group B are approximately of the same order of magnitude as those of group A in the quasi-steady state: 0.08 for $k=0.75$, 0.2 for $k=2.25$ and 0.05 for $k=3.75$ for, example. These large amplitudes then decrease exponentially with time and the amplitudes of the harmonics of group A again are dominant.

The variation of Θ_k^s with time for group A is found to take place in parallel to that of Θ_k^c (Fig. 10) so that

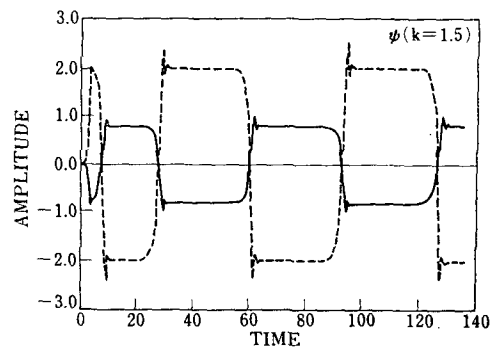

FIG. 11. Same as Fig. 10 except for the streamfunction.

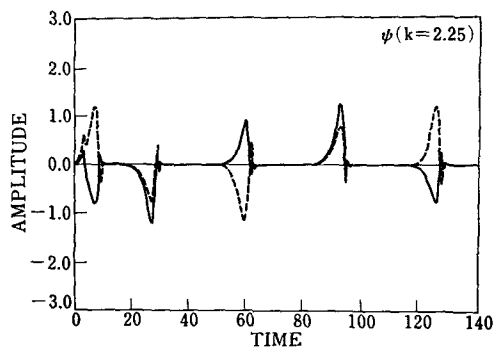

FIG. 13. Same as Fig. 10 except for $k=2.25$ for the streamfunction.

TABLE 2. Spectral density distributions for the temperature field in cases 1 and 3.

Wavenumber	Case 1 (R=1.1 Rc) at $t=180$	Case 3 (R=2 Rc) at $t=110$
0	4.50×10^{-3}	8.91×10^{-3}
0.75	9.03×10^{-16}	2.50×10^{-5}
1.5	1.02×10^{-1}	1.91×10^{-1}
2.25	9.37×10^{-16}	1.00×10^{-4}
3	1.46×10^{-2}	9.96×10^{-2}
3.75	5.55×10^{-16}	4.52×10^{-5}
4.5	7.34×10^{-4}	1.92×10^{-2}
5.25	2.47×10^{-16}	8.35×10^{-6}
6	6.04×10^{-6}	1.02×10^{-3}

the spatial phase of θ_k is approximately (to the first three digits) independent of time through the entire cycle. This is also true for ψ_k, even though $\Psi_k{}^s$ and $\Psi_k{}^c$ have opposite signs all the time (Fig. 11). The phase difference between θ_k and ψ_k is $\pi/2$ for all k in group A. In other words, the harmonics of group A are fixed in space with only the total amplitudes varying with time, and the positive temperature anomaly and the upward motion are in phase.

In contrast to this, the phase of the harmonics of group B vary with time in an interesting fashion. An example is illustrated in Fig. 14 where the phase angles of the harmonic with $k=2.25$ are given as functions of time. It is observed that the phase angles jump by the amount of $\pi/2$ during the short period of time (between $t=97$ and 101 and again between $t=130$ and 134) shortly after the transient stage. During this period, the amplitudes are so small (10^{-5}–10^{-6} at most) that this shift of the phase angle is not reflected in the gross features of the fields.

It is also noted that despite this time variation of phase, the phase difference between θ_k and ψ_k always remains at $\pi/2$ for all k in group B.

The period of time (denoted by τ) for a complete repetition for group A is half of that for group B. In other words, for any amplitude F in group A,

$$F\left(t+\frac{\tau}{2}\right)=F(t),$$

whereas, for group B,

$$F\left(t+\frac{\tau}{2}\right)=-F(t).$$

The variation of the phase with time as described above is responsible for the prolonged period of repetition for group B.

6. Concluding remarks

In this article, extremely regular and repeatable time-dependent convection was found to be a predominant mode for strictly two-dimensional motion in a destabilized fluid layer lying above a stabilized layer for a certain range of Rayleigh number.

As mentioned in the Introduction, a laboratory experiment corresponding qualitatively to the physical situation considered here is being undertaken by Kimura at the Ocean Research Institute of the University of Tokyo. Fig. 15 illustrates one of his experimental results which shows convective flows made visible by time-lapse schlieren photography. The dimentions of his convection tank are 18 cm (length) ×1 cm (width)×4.2 cm (depth), and his fluid is air. The heating is provided by a net of tungsten filaments placed horizontally 1.2 cm above the bottom plate. The arch seen in the photographs is a steel spring used to give sufficient tension to the tungsten filaments. We observe in the photographs that three plumes are present above the net of tungsten filaments (frame a), the middle plume moves to the left and the width of the right-side plume is expanded (frames b and c), the middle plume merges with the left-side plume (frame d), the right-side plume separates to form two plumes (frame e), and three equally spaced plumes are present (frame f). This sequence is then repeated with a period of 47.4 sec.

By changing the experimental parameters such as the rate of heating, and the depths of the destabilized and stabilized layers, Kimura was able to produce many different types of time-dependent convective flows. He also demonstrated that extremely regular and repeatable convection took place in fluids confined

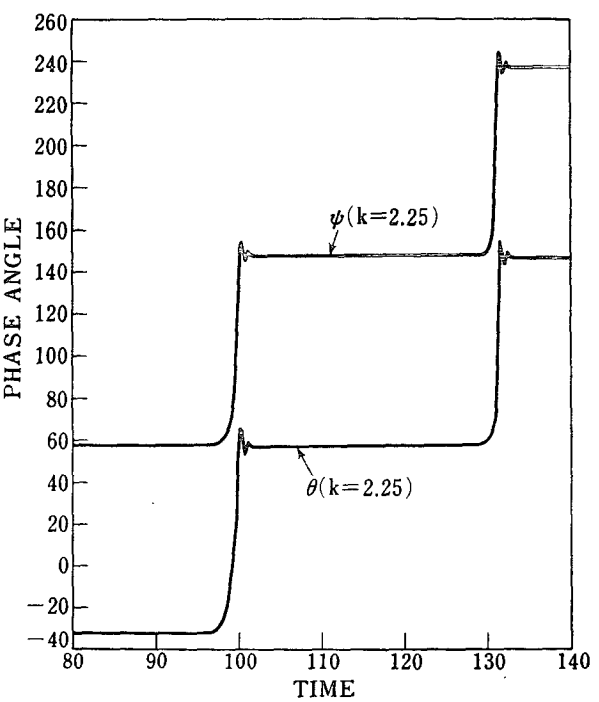

FIG. 14. Variations with time of the phase angles of the harmonics with $k=2.25$ for the temperature deviation and the stream-function for R=2 Rc (case 3).

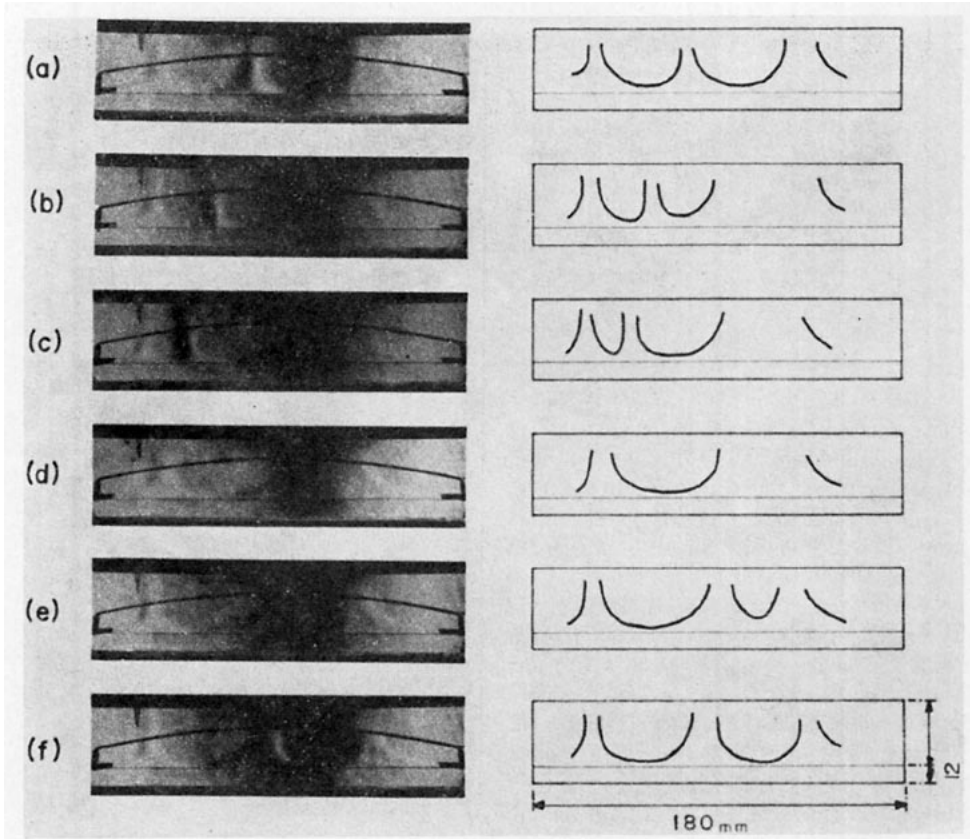

FIG. 15. Schlieren photographs showing evolution of horizontally moving and merging plumes generated by internal heating (Kimura, unpublished). See text for description.

not only in a "two-dimensional" tank where the width is much smaller than the length such as described above, but also in a "three-dimensional" tank.

The present problem may be related to the oscillatory convective motion that takes place in a thin fluid layer heated from below under a physical situation where heat transport increases with the decreasing temperature difference ΔT between the boundaries of the fluid. Busse (1967) considered a situation where the heat flux is the given parameter (rather than ΔT) and where the fluid properties vary appreciably with temperature, and showed that finite-amplitude disturbances can induce convection at Rayleigh numbers smaller than required for infinitesimal perturbations. He found that the heat flux increases with decreasing ΔT just above the Rayleigh number at which convection sets in and that oscillatory states are possible.

A similar conclusion had been reached previously by Veronis (1963, 1965) for the situation where the presence of a stabilizing solute concentration makes the density profile in the fluid curved. Krishnamurti (1968a) also found that changing the heat flux with time can make a multiple-value heating curve possible. Krishnamurti's (1968b) own experiment does show an oscillatory behavior in ΔT. More recently, Caldwell (1970) made a more detailed study on the reversal of slope in the heating curve and oscillations with time. The form of the flow pattern producing the oscillatory temperature signal is not described in these articles, however.

The physical situation considered here has a common feature to those described above: the temperature at the bottom of the destabilized layer is not a prescribed parameter (the temperature distribution in Fig. 1 is introduced simply to represent the effect of internal heating) and the density profile in the fluid is curved. However, it remains unanswered whether or not the physical process producing oscillatory behavior in Krishnamurti's and Caldwell's experiment is also operating in the horizontally moving and merging plumes in our numerical experiment.

In the literature, many different types of convection having time-dependent characters are reported. Several authors have observed time-dependent convective flows in a thin fluid layer bounded by two horizontal plates (Rayleigh convection problem) at high Rayleigh numbers. For example, Willis and Deardorff (1965) observed that well-defined periodic temperature fluctuations appeared approximately at $R \approx 6{,}300$ in air ($Pr = 0.71$) and the fluctuations became quite irregular at $R \approx 10{,}000$ and beyond. They showed later (Willis and Deardorff, 1967) that these two critical Rayleigh numbers at which well-defined unsteady fluctuations and irregular fluctuations appear depend upon the

Prandtl number: as the Prandtl number increases, the critical Rayleigh numbers increase. A later reference of Willis and Deardorff (1970) shows that the oscillations in air are associated with three-dimensional wavelike motions of the basic rolls and are therefore quite different from the two-dimensional time-dependent motions described here. Krishnamurti (1970) also found that the Rayleigh number at which steady convective flow changes to time-dependent flow is approximately 21–31 times the critical Rayleigh number depending upon the Prandtl number for the range of the Prandtl number from 1 to 10^4. In contrast, the periodic convection considered here appears even at the Rayleigh number 1.5 times the critical Rayleigh number.

Another form of convective motion which is periodic in time is the successive generation of thermals over a heated horizontal plate, such as those observed by Sparrow *et al.* (1970). At a given heating rate, thermals are generated at fixed sites which are spaced more or less regularly along the span of the heated surface and the generation of thermals at these sites is periodic in time. A phenomenological theory for this type of flow was presented by Howard (1966) where he envisions the generation of thermals as a break-up phenomenon of the conductive boundary layer adjacent to the heated plate. In contrast, the Rayleigh number considered here is apparently too low for the development of boundary layers at the heated level and therefore the mechanism of generating periodic variations of flows may be different from that described above.

Finally it may be noted that oscillatory temperature variations are quite characteristic of thermally induced convection in liquid metal systems containing vertical or horizontal temperature gradients. The latest reference in this area includes an article by Verhoeven (1969) who reports that the first oscillatory mode appears at a Rayleigh number 10% higher than the critical Rayleigh number for the outset of fluid flow predicted by linear stability theory, and the second oscillatory mode, having a shorter period, begins at Rayleigh numbers 30% above the critical value.

Acknowledgments. The authors wish to thank Mr. Ryuji Kimura for permitting use of his photographs before publication of his paper, Dr. Marvin A. Geller for reading the manuscript, and Mrs. Sandy Bryant for typing the manuscript.

This work was sponsored by the Atmospheric Sciences Section, National Science Foundation, under Grant GA-20328. The computations were made on the Control Data Corporation 6600 computer at the National Center for Atmospheric Research which is sponsored by the National Science Foundation.

REFERENCES

Busse, F. H., 1967: Non-stationary finite amplitude convection. *J. Fluid Mech.*, **28**, 223–239.

Caldwell, D. R., 1970: Non-linear effects in a Rayleigh-Bénard experiment. *J. Fluid Mech.*, **42**, 161–176.

Foster, T. D., 1969: The effect of initial conditions and lateral boundaries on convection. *J. Fluid Mech.*, **37**, 81–94.

Gribov, V. N., and L. E. Gurevich, 1957: On the theory of stability of a layer located at a superadiabatic temperature gradient in a gravitational field. *Soviet Phys. JETP*, **4**, 720–729.

Howard, L. N., 1966: Convection at high Rayleigh number. *Proceedings 11th International Congress Applied Mechanics*, Berlin, Springer, 1109–1115.

Koschmieder, E. L., 1969: On the wavelength of convective motions. *J. Fluid Mech.*, **35**, 527–530.

Krishnamurti, R., 1968a: Finite-amplitude convection with changing mean temperature. Part I. Theory. *J. Fluid Mech.*, **33**, 445–455.

——, 1968b: Finite amplitude convection with changing temperature. Part 2. An experimental test of the theory. *J. Fluid. Mech.*, **33**, 457–463.

——, 1970: On the transition to turbulent convection. Part 2. The transition to time-dependent flow. *J. Fluid. Mech.*, **42**, 309–320.

Lilly, D. K., 1964: Numerical solutions for the shape-preserving two-dimensional thermal convection element. *J. Atmos. Sci.*, **21**, 83–98.

Martin B. W., 1967: Free convection in a vertical cylinder with internal heat generation. *Proc. Roy. Soc. London*, **A301**, 327–341.

Ogura, M., 1969: A direct solution of Poisson's equation by dimension reduction method. *J. Meteor. Soc. Japan*, **47**, 319–323.

Ogura, Y. 1971: A numerical study of wavenumber selection in finite-amplitude Rayleigh convection. *J. Atmos. Sci.*, **28**, 709–717.

——, and H. Kondo, 1970: A linear stability of convective motion in a thermally unstable layer below a stable region. *J. Meteor. Soc. Japan*, **48**, 204–215.

——, and A. Yagihashi, 1969: A numerical study of convection rolls in a flow between horizontal parallel plates. *J. Meteor. Soc. Japan*, **47**, 205–218.

——, and ——, 1970: A numerical study of finite-amplitude time-dependent convection induced by time-independent internal heating: Truncated systems. *J. Meteor. Soc. Japan*, **48**, 1-17.

Richtmyer, R. D., and K. W. Morton, 1967: *Difference Methods for Initial-Value Problems*, 2nd ed. New York, Interscience Publ., 405 pp.

Rintel, L., 1967: Penetrative convective instabilities. *Phys. Fluids*, **10**, 848–854.

Sparrow, E. M., R. B. Husar and R. J. Goldstein, 1970: Observations and other characteristics of thermals. *J. Fluid Mech.*, **41**, 793–800.

Todd, J., 1962: *Survey of Numerical Analysis*. New York, McGraw-Hill, 582 pp.

Verhoeven, J. D., 1969: Experimental study of thermal convection in a vertical cylinder of mercury heated from below. *Phys. Fluids*, **12**, 1733–1739.

Veronis, G., 1963: Penetrative convection. *Astrophys. J.*, **137**, 641–663.

——, 1965: On finite-amplitude instability in thermohaline convection. *J. Marine Res.*, **23**, 1–17.

Watson, A., 1966: Natural convection in a closed vertical cylinder containing a heat-generating fluid. Ph.D. thesis, London University.

Whitehead, J. A., and M. M. Chen, 1970: Thermal stability and convection of a thin fluid layer bounded by a stably stratified region. *J. Fluid Mech.*, **40**, 549–576.

Willis, G. E., and J. W. Deardorff, 1965: Measurements on the development of thermal turbulence in air between horizontal plates. *Phys. Fluids*, **8**, 2225–2229.

——, and——, 1967: Development of short-period temperature fluctuations in thermal convection. *Phys. Fluids*, **10**, 931–937.

——, and ——, 1970: The oscillatory motions of Rayleigh convection. *J. Fluid Mech.*, **44**, 661–672.